Chemical Physics Letters 513 (2011) 179–183

Contents lists available at SciVerse ScienceDirect

Chemical Physics Letters

journal homepage: www.elsevier.com/locate/cplett

Theoretical calculations of the excited state potential energy surfaces of nitric oxide

Olga V. Ershova, Nicholas A. Besley *

School of Chemistry, University of Nottingham, University Park, Nottingham NG7 2RD, UK

ARTICLE INFO

Article history:
Received 16 June 2011
In final form 27 July 2011
Available online 2 August 2011

ABSTRACT

Excited state potential energy surfaces of NO are studied using density functional theory and coupled cluster theory exploiting a recently developed algorithm called the maximum overlap method. States arising from excitation to Rydberg orbitals are described well, with coupled cluster theory providing properties comparable in accuracy to multi-reference configuration interaction calculations. For the $\pi \rightarrow \pi^*$ valence states, larger errors are observed with density functional theory, and coupled cluster theory fails. This is associated with the multiconfigurational nature of these states. The calculations yield pseudo diabatic states, allowing the surface crossing between the $B^2\Pi$ and $C^2\Pi$ states to be studied directly.

1. Introduction

Nitric oxide (NO) is important in many chemical and biological processes. These include, the formation of smog and acid rain, the depletion of ozone in the atmosphere and it has a role in the control of blood circulation, nerve transmission and the functioning of the immune system [1]. Understanding the electronic structure of NO is critical for the ability to model and predict the activity of NO and its interaction with other molecules at a molecular level. Interest in NO is enhanced further by its spatially degenerate open-shell electronic structure, which represents a challenge to theoretical methods, making NO an informative and challenging molecule to test electronic structure theories.

The ground and excited states of NO have been the subject of a wide range of experimental investigations. A summary of much of this work can be found elsewhere [2]. More recently, the interaction between NO in different excited states with atoms and molecules has been studied [3]. NO has low-lying Rydberg and valence states. The Rydberg states are characterized by ω_e and B_e values that are similar to NO^+, while the valence states show an increase in bond length compared to the ground state and lower values of ω_e [4]. Experimental values for the main spectroscopic parameters of the low-lying states of NO are shown in Table 1.

Several authors have studied the excited states of NO with the multi-reference configuration interaction (MRCI) method [5–7]. In a key contribution, de Vivie and Peyerimhoff used MRCI to compute potential energy surfaces for a large number of low-lying doublet and quartet excited states of NO and reported an average error of about 1300 cm^{-1} in the computed adiabatic excitation energies [6]. Subsequently, more extensive MRCI calculations were reported for a slightly smaller set of excited states that reproduced the experimental bond lengths (r_e), rotational constants (B_e), excitation energies (T_e) and vibrational frequencies (ω_e) with errors of 0.012 Å, 0.026 cm^{-1}, 620 cm^{-1} and 41 cm^{-1}, respectively [7]. Another study focused on the $A^2\Sigma^+$ and $D^2\Sigma^+$ states, reporting MRCI calculations of the dipole moment and electric field gradients at the nuclei [8]. These studies demonstrate that accurate potential energy curves can be obtained using the MRCI method in conjunction with a large active space and extensive basis set.

One feature of the excited state potential energy surfaces of NO is an avoided crossing between the $C^2\Pi$ and $B^2\Pi$ states, which occurs at a bond length close to that of the ground state. Several studies have computed the precise location of this avoided crossing. In the work of de Vivie-Riedle et al. [9], the computed adiabatic states were transformed to a diabatic representation and the crossing was found to lie at bond length of 1.17 Å with an energy of 57 000 cm^{-1}. In the MRCISD+Q calculations of Shi and East [7], values of 1.18 Å and 57 623 cm^{-1} were estimated from the adiabatic potential energy curves. In a different approach, the surface crossing was studied using an *ab initio* *R*-matrix technique combined with multi-channel quantum defect theory [10]. This work found slightly different values of 1.25 Å and 60 000 cm^{-1} for the location of the surface crossing.

While MRCI can characterize the excited states of NO successfully, its computational cost can inhibit its application to study complexes of NO with other molecules. In this Letter, we explore the calculation of the excited state potential energy surfaces of NO with alternative methods based on density functional theory (DFT) and coupled cluster theory that can be more readily applied to larger systems. In particular, we focus on self consistent field (SCF) based methods exploiting a technique that allows the application of these methods to study excited states.

* Corresponding author. Fax: +44 115 951 3562.
E-mail address: nick.besley@nottingham.ac.uk (N.A. Besley).

0009-2614/$ - see front matter © 2011 Elsevier B.V. All rights reserved.
doi:10.1016/j.cplett.2011.07.089

Table 1
Experimental values for the main spectroscopic parameters of the excited states of NO. All values taken from reference [4] except [a]reference [31], [b]reference [32] and [c]reference [33]. Absolute errors in ω_e and T_e should not exceed 1 cm^{-1} and absolute errors in r_e should not exceed 0.001 Å (except for the L' state, for which the error is 0.003 Å).

State	T_e (cm^{-1})	r_e (Å)	ω_e (cm^{-1})
$X^2\Pi$	–	1.151	1904
$A^2\Sigma^+$	43966	1.063	2374
$C^2\Pi$	52126	1.062	2395
$D^2\Sigma^+$	53085	1.062	2324
$a^4\Pi^a$	38711	1.422	1016
$B^2\Pi$	45914	1.417	1037
$b^4\Sigma^{-a}$	46492	1.289	1262
$L'^2\Phi^b$	53676	1.422	1000
$L^2\Pi^c$	62028	1.399	975

2. Computational details

Excited state potential energy surfaces have been computed using time-dependent density functional theory (TDDFT). For a detailed account of the formalism and implementation of TDDFT, the reader is referred to a recent review [11]. In this study we have used the hybrid exchange–correlation functional B3LYP [12,13] and the long-range corrected exchange–correlation functional ωB97X [14]. These functionals were chosen to represent standard hybrid and Coulomb attenuated functionals. To reduce errors arising from the numerical integration, a 100 point Euler–Maclaurin combined with 194 point Lebedev integration grid was used. Potential energy surfaces were also computed with the equations of motion coupled cluster (EOM-CCSD) method [15]. Λ doubling was not accounted for since it is of the order of 100 cm^{-1} or less [9].

TDDFT and EOM-CCSD are based on the response of the ground state orbitals to an electric field. Excited states can also be studied within Kohn–Sham DFT or coupled cluster theory by exploiting techniques that force the SCF calculation to converge to higher energy roots of the Kohn–Sham or Hartree–Fock equations [16–18]. An advantage of such approaches is that the orbitals are directly optimized to describe the excited state of interest. This allows excitation energies to be determined in a ΔSCF approach, wherein the excitation energy is the difference between the excited state and ground state energies. In this work, a procedure called the maximum overlap method (MOM) is used [16,18]. In contrast to standard SCF calculations, where the lowest energy orbitals are occupied, the MOM approach yields excited state solutions by defining an alternative set of occupied orbitals. These orbitals are chosen to be those that overlap most with the *span* of the orbitals that were occupied on the previous SCF cycle. The new occupied orbitals are identified by defining an orbital overlap matrix

$$\mathbf{O} = (\mathbf{C}^{\text{old}})^{\dagger}\mathbf{S}\mathbf{C}^{\text{new}} \tag{1}$$

O_{ij} gives the overlap between the ith old orbital and the jth new orbital and the projection of the jth new orbital onto the old occupied space is

$$p_j = \sum_{i}^{n} O_{ij}^2 \tag{2}$$

where

$$O_{ij} = \sum_{\nu}^{N}\left[\sum_{\mu}^{N} C_{\mu i}^{\text{old}} S_{\mu\nu}\right] C_{\nu j}^{\text{new}} \tag{3}$$

The n occupied orbitals are chosen to be the ones with the largest projections p_j. Thus if a SCF calculation is started with orbitals that describe an excited state, the MOM procedure will allow the SCF calculation to variationally optimize the orbitals whilst preventing the variational collapse to the ground state. The initial orbitals are typically generated by modifying the occupancies of the molecular orbitals obtained from a calculation on the ground state. Even with the MOM procedure, SCF calculations can still collapse to given a lower lying state. However, it is often possible to obtain such states by starting the SCF calculation with different orbitals. Single determinant based methods are well known to provide an incorrect description of open-shell singlet states [19]. However, for the predominantly doublet excited states of NO such approaches have the potential to provide an accurate description [20].

The MOM approach has been used in conjunction with DFT with the B3LYP and ωB97X functionals, CCSD and CCSD(T) methods. For some states, applying CCSD to the excited state determinant led the calculation to diverge. In an excited state determinant generated using the MOM approach there is likely to be a virtual orbital with a lower energy than one or more of the occupied orbitals. In some cases, the coupled cluster amplitude for configurations generated by de-excitation into this low lying orbital to give the ground state grows rapidly, and the energy rapidly tends to infinity. Preventing these amplitudes from becoming too large by scaling the coupled cluster amplitudes, by typically 0.5–0.25, during the early iterations of the CCSD calculation can avoid this problem and allow the calculation to converge. After the initial few iterations (typically 10) the CCSD calculation proceeds with no restrictions or modifications, and so the final energy is not affected.

For the $A^2\Sigma^+$ and $C^2\Pi$ states, the starting orbitals were generated by modifying the occupancies from the ground state with a bond length of 1.05 Å. This approach applied to the $D^2\Sigma^+$ results in a variational collapse to give the $A^2\Sigma^+$ state. This state is obtained by modifying the occupancies of the orbitals from the $A^2\Sigma^+$ state. The valence $\pi\pi^*$ states were generated by modifying the occupancies of the ground state orbitals for a bond length of 1.41 Å. The d-aug-cc-pVTZ basis set [21,22] was used for calculations of the Rydberg states, and the aug-cc-pVTZ basis set was used for valence state calculations. For these valence states, the additional diffuse functions have no significant effect on the properties of the excited states. All calculations were performed with the Q-Chem software package [23], and the potential energy surfaces were fitted to a 4th power Taylor series in the vicinity (within 21 points with a separation of 0.002 Å) of the minima to determine the spectroscopic parameters.

3. Results

3.1. Rydberg states

Table 2 shows the computed properties for the Rydberg states $A^2\Sigma^+$, $C^2\Pi$ and $D^2\Sigma^+$ which correspond to excitation of the unpaired electron in the π^* orbital to $3s$, $3p_\pi$ and $3p_\sigma$ orbitals, respectively, using a range of methods including TDDFT and EOM-CCSD. As expected TDDFT with the B3LYP exchange–correlation functional underestimates the excitation energies for the Rydberg excitations. This deficiency of standard hybrid functionals is understood and well documented in the literature [24–26]. With the long-range corrected ωB97X functional there is a significant improvement in the computed excitation energies, although they remain too low, and an error of about 5000 cm^{-1} (0.6 eV) compared with experiment is disappointingly large. Beyond the calculation of excitation energies it is also of interest to determine how well the different methods predict the shape of the potential energy surfaces for the different states, which can be inferred from the calculated bond lengths and vibrational

Table 2
Error in the computed spectroscopic properties for the Rydberg states with the d-aug-cc-pVTZ basis set.

State	Method	T_e (cm^{-1})	r_e (Å)	ω_e (cm^{-1})
$A^2\Sigma^+$	TD-B3LYP	−7232	−0.008	53
	TD-ωB97X	−3206	−0.010	180
	EOM-CCSD	−858	−0.005	100
	MOM-B3LYP	2160	−0.006	107
	MOM-ωB97X	3631	−0.009	160
	MOM-CCSD	−351	−0.007	124
	MOM-CCSD(T)	−705	0.002	19
	MRCISD+Q[a]	−408	0.008	−30
$C^2\Pi$	TD-B3LYP	−9457	−0.008	−65
	TD-ωB97X	−5262	−0.010	188
	EOM-CCSD	−955	−0.006	88
	MOM-B3LYP	1252	−0.009	110
	MOM-ωB97X	2446	−0.010	160
	MOM-CCSD	−429	−0.008	120
	MOM-CCSD(T)	−695	0.001	8
	MRCISD+Q[a]	−318	0.006	−67
$D^2\Sigma^+$	TD-B3LYP	−10925	−0.012	106
	TD-ωB97X	−5255	−0.007	217
	EOM-CCSD	−897	−0.002	107
	MOM-B3LYP	1292	−0.002	94
	MOM-ωB97X	2590	−0.006	174
	MOM-CCSD	−453	−0.003	130
	MOM-CCSD(T)	−742	0.006	14
	MRCISD+Q[a]	−593	0.012	−1

[a] Reference[7].

frequencies. The accuracy of the predicted bond lengths are similar between the two functionals, consistent with earlier work [14]. However, the predicted vibrational frequencies are better with B3LYP. While the ωB97X functional was parameterized using a range of ground state properties, these did not include vibrational frequencies. EOM-CCSD shows a marked improvement on the TDDFT calculations. The errors in the excitation energies are reduced to less than 1000 cm^{-1} (0.12 eV). This remains higher than the values for the larger MRCI calculations [7], but still represents a good level of accuracy. The predicted bond lengths are comparable to, or more accurate than MRCI, while greater errors are observed for the vibrational frequencies.

The excitation energies predicted by the ΔSCF based DFT methods are closer to experiment than those from TDDFT. In particular, B3LYP provides quite accurate values for T_e, r_e and ω_e, which are consistently better than with ωB97X. Coupled cluster theory gives a further increase in accuracy. The MOM-CCSD excitation energies are closer to experiment and comparable to MRCI. However, this is slightly fortuitous since there is a greater deviation from experiment when the triples correction is used. MOM-CCSD(T) gives excitation energies with an error of less than 800 cm^{-1} (0.1 eV), representing a high level of accuracy. The inclusion of the triples correction results in a significant improvement in r_e and ω_e highlighting the importance of the triples correction for very accurate surfaces. Overall, the accuracy of MOM-CCSD(T) is comparable to or better than MRCI for the Rydberg states. In the calculations of Shi and East [7], an active space comprising the full valence space plus 3*s* and 3*p* Rydberg orbitals, with the core 1*s* orbitals of nitrogen and oxygen kept doubly occupied, was used. Using the MOLPRO software [27], a calculation using this active space with the aug-cc-pVTZ basis set takes several minutes using a single Intel XEON processor while a CCSD(T) calculation takes between 10 and 20 s. Furthermore, advances in local correlation coupled cluster methods have resulted in a much more favourable scaling with system size [28], making CCSD(T) calculations applicable to larger complexes containing NO.

3.2. Valence states

Table 3 shows results for the low lying quartet valence states computed with the aug-cc-pVTZ basis set. For these states, there is little difference between the results obtained with singly and doubly augmented basis sets. For the lower energy $a^4\Pi$ state the MOM procedure and TDDFT are not required because it is the lowest energy state of its spin state and can be studied directly within Kohn–Sham DFT or CCSD(T). For this state, all the methods provide relatively accurate spectroscopic parameters, with CCSD(T) providing particularly close to experiment. Overall, for the $b^4\Sigma^-$ state, the TDDFT and EOM-CCSD calculations have larger errors than the ΔSCF based approaches and also the errors for the $a^4\Pi$ state. In the TDDFT and EOM-CCSD calculations shown here, the quartet states have been computed using the ground doublet state as a reference. It is possible that better results may be obtained from using the $a^4\Pi$ state as a reference. The results for the ΔSCF based methods are similar to those observed for the Rydberg states. MOM-B3LYP has higher errors for the excitation energy, but describes the shape of the potential energy surfaces, as given by r_e and ω_e, better than the ωB97X functional. For both states there is a large improvement with (MOM)-CCSD and (MOM)-CCSD(T), in particu-

Table 3
Error in the computed spectroscopic properties for the valence quartet states with the aug-cc-pVTZ basis set. For the $a^4\Pi$ state the MOM procedure is not required.

State	Method	T_e (cm^{-1})	r_e (Å)	ω_e (cm^{-1})
$a^4\Pi$	B3LYP	−2092	0.001	34
	ωB97X	−1293	−0.021	109
	CCSD	−1906	−0.014	58
	CCSD(T)	−521	−0.001	11
	MRCI[a]	−3050	0.029	−86
$b^4\Sigma^-$	TD-B3LYP	1839	−0.004	28
	TD-ωB97X	4109	−0.015	109
	EOM-CCSD	4746	−0.018	100
	MOM-B3LYP	−2005	−0.004	27
	MOM-ωB97X	−1204	−0.016	86
	MOM-CCSD	−774	−0.007	1
	MOM-CCSD(T)	−403	0.001	4
	MRCI[a]	−1135	0.029	−51

[a] Reference[6].

Table 4
Error in the computed spectroscopic properties for the valence states with the aug-cc-pVTZ basis set.

State	Method	T_e (cm^{-1})	r_e (Å)	ω_e (cm^{-1})
$B^2\Pi$	TD-B3LYP	−2148	−0.056	703
	TD-ωB97X	521	−0.083	877
	EOM-CCSD	−587	−0.040	182
	MOM-B3LYP	−4200	−0.010	−3
	MOM-ωB97X	−2328	−0.013	73
	MRCISD+Q[a]	−1111	0.010	71
$L'^2\Phi$	TD-B3LYP	9700	−0.057	748
	TD-ωB97X	11083	−0.083	932
	EOM-CCSD	8686	−0.042	227
	MOM-B3LYP	4115	0.014	5
	MOM-ωB97X	4948	−0.008	77
	MRCISD+Q[a]	−701	0.017	−24
$L^2\Pi$	TD-B3LYP	−6552	−0.001	570
	TD-ωB97X	−4453	−0.029	692
	EOM-CCSD	−8122	−0.018	228
	MOM-B3LYP	−3256	0.006	126
	MOM-ωB97X	−323	−0.025	252
	MRCISD+Q[a]	−902	0.051	−22

[a] Reference[7].

lar the addition of the triples correction is significant. For both states, the results for CCSD(T) are significantly closer to experiment than MRCI [6]. It should be noted, however, that the MRCI results for the quartet states pertain to the earlier work of Peyerimhoff and more accurate results from MRCI would be obtained using the more extensive MRCI approach reported by Shi and East, who did not consider the quartet states.

Results of calculations for the doublet $\pi \rightarrow \pi^*$ states $B^2\Pi$, $L'^2\Phi$ and $L^2\Pi$ are given in Table 4. These states are known to be a mixture of $\pi_x^1\pi_y^2\pi_y^{*2}$, $\pi_x^1\pi_y^2\pi_x^{*2}$ and $\pi_x^1\pi_y^2\pi_x^{*1}\pi_y^{*1}$ configurations [6] and

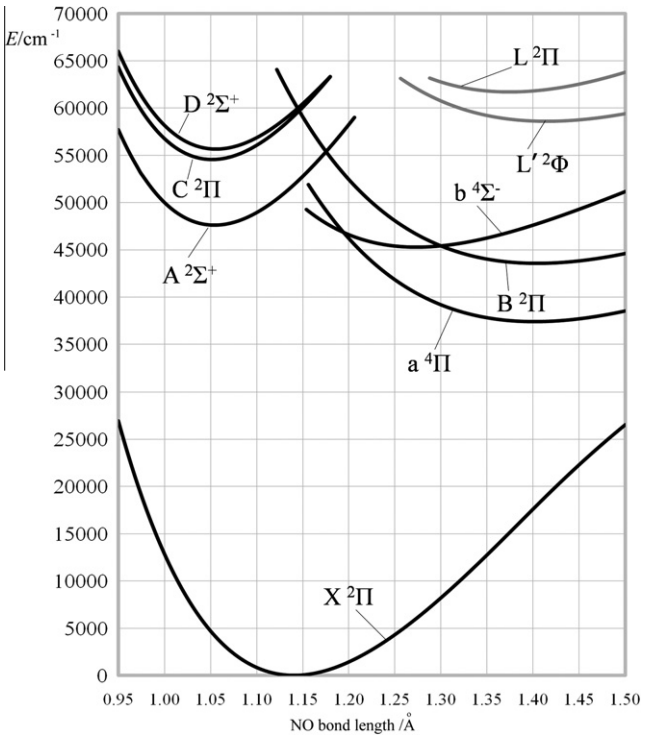

Figure 1. Calculated MOM-ωB97X potential energy surfaces. Rydberg states computed with the d-aug-cc-pVTZ basis set, valence and ground states computed with the aug-cc-pVTZ basis set.

are not well suited to single reference based approaches. For these states there is a small energy separation between the different components of the $L'^2\Phi$ and $L^2\Pi$ states states resulting in a loss in degeneracy. This energy separation is small and we present results for the state that is closest to the experimental T_e. However, this does not affect the conclusions regarding accuracy of the different methods. For the MOM based calculations, large errors in the computed excitation energies are obtained using the B3LYP functional, with T_e underestimated for the $B^2\Pi$ and $L^2\Pi$ states, and overestimated for the $L'^2\Phi$ state. This results in the $L'^2\Phi$ and $L^2\Pi$ states being much too close in energy. Despite an overall improvement in the excitation energies with the ωB97X functional, the $L'^2\Phi$ and $L^2\Pi$ states remain too close in energy. However, for both functionals, the predicted r_e and ω_e are in reasonable agreement with experiment. The set of potential energy curves computed with MOM-ωB97X are shown in Figure 1 and illustrate the problems for the calculation of the valence states. While the $B^2\Pi$, $L'^2\Phi$ and $L^2\Pi$ states should be evenly spaced in energy, the $L'^2\Phi$ and $L^2\Pi$ states are much too close together.

The overestimation of the excitation energy for the $L'^2\Phi$ state and underestimation for the $L^2\Pi$ state is greater for the TDDFT calculations and this results in the ordering of these states to be incorrect. More severe problems are evident in the coupled cluster calculations where no minimum is observed for bond lengths in the region 1.37–1.47 Å. This is most likely linked to the increasing importance of non-dynamic correlation and the Hartree–Fock wavefunction being a poor reference for these states. Overall, all of the single determinant based approaches provide a poor description of these states, particularly the $L'^2\Phi$ and $L^2\Pi$ states, suggesting that for these states a multireference based approach is required.

3.3. $C^2\Pi$ and $B^2\Pi$ surface crossing

For the $B^2\Pi$ and $C^2\Pi$ states, MRCI calculations will provide adiabatic states that do not cross. Diabatic states can be generated through a unitary transformation applied to the adiabatic states [9]. Recently, the constrained DFT method has been developed and shown to give pseudo diabatic states directly without requiring the calculation of adiabatic states [29]. The MOM approach also gives pseudo diabatic states directly and does not require any partitioning of the system under consideration. Since the states are

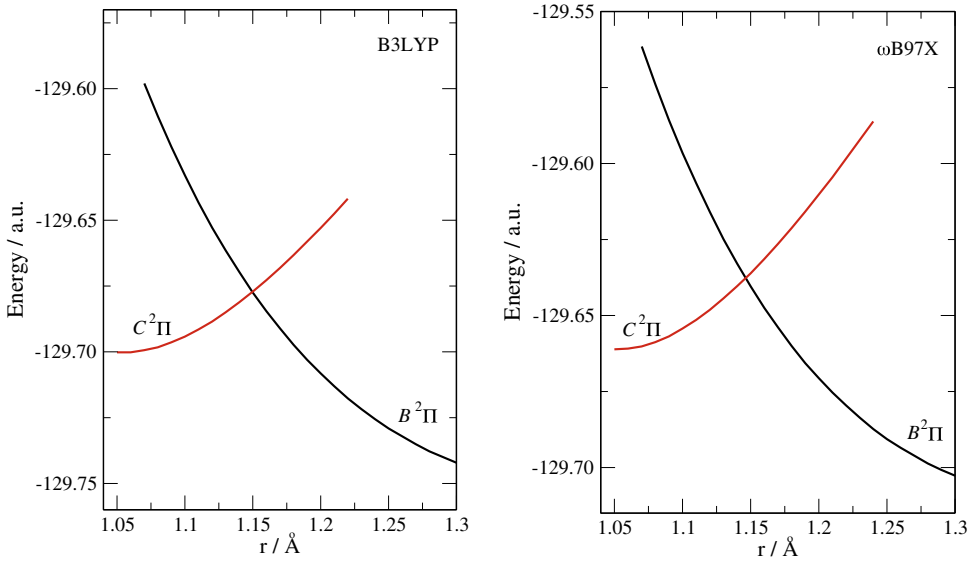

Figure 2. Calculated surface crossing of the $B^2\Pi$ and $C^2\Pi$ states with MOM-B3LYP and MOM-ωB97X in conjunction with the d-aug-cc-pVTZ basis set.

Table 5
Mean absolute deviation in computed excitation energies, equilibrium bond lengths and vibrational frequencies from experiment.

Method	T_e (cm^{-1})	r_e (Å)	ω_e (cm^{-1})
MOM-B3LYP	2547	0.007	63
MOM-ωB97X	2345	0.014	136
MOM-CCSD(T)[b]	613	0.002	11
MRCI[a]	1027	0.020	44

[a] Reference[7,6].
[b] Excluding $B^2\Pi$, $L'^2\Phi$ and $L^2\Pi$ states.

computed in separate SCF calculations, they will be eigenfunctions of slightly different Hamiltonians and therefore are able to intersect. Figure 2 shows computed surfaces for the $B^2\Pi$ and $C^2\Pi$ states with B3LYP and ωB97X functionals and d-aug-cc-pVTZ basis set. The states cross at a bond lengths of 1.150 and 1.146 Å for B3LYP and ωB97X at energies of 58457 cm^{-1} and 59657 cm^{-1}, respectively. These values are in good agreement with values obtained from MRCI [9]. Both functionals give crossing points that are at a slightly smaller bond length. This is likely to be improved by the presence of more diffuse basis functions which will preferentially lower the energy of the $C^2\Pi$ state and result in a crossing point at a larger bond length. Unfortunately, such a surface crossing point cannot be determined from the coupled cluster calculations due its failure for the $B^2\Pi$ state.

4. Conclusions

Previous work [6,7] has shown that accurate excited state potential energy surfaces for NO can be computed with extensive MRCI calculations. In this study, we have investigated the application of computationally less expensive methods to this problem. Two general approaches to computing excited states have been studied, those based on response theory and those wherein the SCF procedure is forced to converge to an excited state. For the Rydberg and quartet valence states, the MOM-based approaches provide a good description of the excited states. Overall, for the DFT calculations with the two exchange–correlation functionals considered, the MOM based approaches perform comparable to or better than TDDFT. The mean absolute deviation from experiment for these methods is shown in Table 5. The predicted excitation energies are better with MOM-ωB97X, but equilibrium bond lengths and vibrational frequencies are significantly better with MOM-B3LYP. On average, an error of approximately 2500 cm^{-1} (0.3 eV) is observed in the excitation energies. In particular, for the Rydberg and quartet valence states, the MOM-CCSD(T) method provides excellent agreement with experiment, which is comparable to extensive MRCI calculations. The two functionals considered here cannot represent fully recent developments in exchange–correlation functionals. Alternative long-range corrected functionals or the recent functionals of Truhlar [30] could certainly improve the accuracy of the DFT calculations presented here, although it is unlikely that they would match the accuracy of the MOM-CCSD(T) or MRCI calculations.

For the doublet valence $\pi \rightarrow \pi^*$ states the MOM-CCSD(T) calculations failed to produce correct potential energy surfaces. The MOM-DFT calculations gave surfaces with a reasonable shape but did not correctly reproduce the energy spacings between the states, in particular the $L'^2\Phi$ and $L^2\Pi$ states. The reason for this failure is probably associated with the genuine multiconfigurational character of these states and indicates that these approaches are not suitable for states of this nature. Another important property of the MOM based calculations is that diabatic states can be determined directly. The surface crossing between the $B^2\Pi$ and $C^2\Pi$ states has been characterized and shown to be consistent with previous studies using MRCI.

Acknowledgments

This work is supported by the Engineering and Physical Sciences Research Council (EP/H004815). We are grateful for access to the University of Nottingham High Performance Computer and to Prof. Tim Wright and Dr. Richard Wheatley for useful discussions.

References

[1] T. Nagano, T. Yoshimura, Chem. Rev 102 (2002) 1235.
[2] E. Miescher, K.P. Huber, International Review of Science, Physical Chemistry Series 2, vol. 3, Spectroscopy, Butterworths, London, 1976.
[3] Y. Kim, H. Meyer, Int. Rev. Phys. Chem 20 (2001) 219.
[4] K.P. Huber, G. Herzberg, Molecular Spectra and Molecular Structure IV Constants of Diatomic Molecules, Van Nostrand, New York, 1979.
[5] F. Grein, A. Kapur, J. Chem. Phys 77 (1982) 415.
[6] R. de Vivie, S.D. Peyerimhoff, J. Chem. Phys 89 (1988) 3028.
[7] H. Shi, A.L. L East, J. Chem. Phys 125 (2006) 104311.
[8] R. Polák, J. Fišer, Chem. Phys. Lett 377 (2003) 564.
[9] R. de Vivie, M.C. van Hemert, S.D. Peyerimhoff, J. Chem. Phys 92 (1990) 3613.
[10] M. Hiyama, M.S. Child, J. Phys. B 35 (2002) 1337.
[11] A. Dreuw, M. Head-Gordon, Chem. Rev 105 (2005) 4009.
[12] A.D. Becke, J. Chem. Phys. 98 (1993) 5648.
[13] P.J. Stephens, F.J. Devlin, C.F. Chabalowski, M.J. Frisch, J. Phys. Chem. 98 (1994) 11623.
[14] J.-D. Chai, M. Head-Gordon, J. Chem. Phys. 128 (2008) 084106.
[15] J.F. Stanton, R.J. Bartlett, J. Chem. Phys. 98 (1993) 7029.
[16] A.T.B. Gilbert, N.A. Besley, P.M.W. Gill, J. Phys. Chem. A 112 (2008) 13164.
[17] A.J.W. Thom, M. Head-Gordon, Phys. Rev. Lett. 101 (2008) 193001.
[18] N.A. Besley, A.T.B. Gilbert, P.M.W. Gill, J. Chem. Phys. 130 (2009) 124308.
[19] I. Frank, J. Hutter, D. Marx, M. Parrinello, J. Chem. Phys. 108 (1998) 4060.
[20] D. Robinson, N.A. Besley, Phys. Chem. Chem. Phys. 12 (2010) 9667.
[21] T.H. Dunning Jr., J. Chem. Phys. 90 (1989) 1007.
[22] R.A. Kendall, T.H. Dunning Jr., R.J. Harrison, J. Chem. Phys. 96 (1992) 6796.
[23] Y. Shao et al., Phys. Chem. Chem. Phys. 8 (2006) 3172.
[24] D.J. Tozer, N.C. Handy, J. Chem. Phys. 109 (1998) 10180.
[25] M.E. Casida, D.R. Salahub, J. Chem. Phys. 113 (2003) 8918.
[26] D.J. Tozer, N.C. Handy, Mol. Phys. 101 (2003) 2669.
[27] MOLPRO, version 2010.1, a package of ab initio programs, H-J. Werner, P.J. Knowles, G. Knizia, F.R. Manby, M. Schütz, et al., 2010. Available from: <www.molpro.net>.
[28] C. Hampel, H.-J. Werner, J. Chem. Phys. 104 (1996) 6286.
[29] T. Van Voorhis, T. Kowalczyk, B. Kaduk, L.-P. Wang, C.-L. Cheng, Q. Wu, Annu. Rev. Phys. Chem. 61 (2010) 149.
[30] Y. Zhao, D.G. Truhlar, Acc. Chem. Res. 41 (2008) 157.
[31] K.P. Huber, M. Vervloet, J. Mol. Spectrosc. 129 (1988) 1.
[32] M.R. Taherian, P.C. Cosby, T.G. Slanger, J. Chem. Phys. 83 (1985) 3878.
[33] K. Dressler, E. Miescher, J. Chem. Phys. 75 (1981) 4310.